INTERACTION OF LASER RADIATION WITH A TARGET

Tomographic imaging of a target directly irradiated in experiments on the Iskra-5 iodine laser facility

S.V. Bondarenko, R.V. Garanin, S.G. Garanin, N.V. Zhidkov,
O.V. Oreshkov, S.V. Potapov, N.A. Suslov, N.V. Frolova

Abstract. **We set forth the data of experiments involving direct microtarget irradiation by the 12 second-harmonic beams ($\lambda = 0.66$ μm) of iodine laser radiation carried out on the Iskra-5 facility. For microtargets we employed glass shells ~ 500 μm in diameter with ~ 1-μm thick walls, which were filled with a DT mixture at a pressure $p_{DT} \approx 3 - 4$ atm. In one of these experiments, a tomographic image of the microtarget was recorded from the images obtained using pinhole cameras, which were arranged along seven different directions. The pinhole images were acquired in the X-ray radiation with photon energies above 1.5 keV. The procedure used for reconstructing the volume luminosity of the microtarget is described. An analysis of the tomographic image suggests that the compressed microtarget domain possesses a complex asymmetric shape; $20 - 30$ μm sized structural elements being clearly visible. The resultant data set allowed us to estimate the initial nonuniformity of microtarget surface irradiation by the laser radiation. The rms nonuniformity of microtarget irradiance was estimated at $\sim 60\%$.**

1. Introduction

As is well known, to ignite thermonuclear reactions in a DT fuel requires compressing it to a high density, $\sim 10^3$ times the liquid density [1]. The key problem in the attainment of such a high density is to ensure a high symmetry of shell implosion. Information about the symmetry of shell implosion as well as about the shape and uniformity of compressed fuel is ordinarily acquired from target images in corpuscular or, more frequently, X-ray radiation. However, a single image of this kind allows obtaining only the two-dimensional distribution of the characteristics of an object integrated along the observation direction. Three-dimen-

**S.V. Bondarenko, R.V. Garanin, S.G. Garanin, N.V. Zhidkov,
O.V. Oreshkov, S.V. Potapov, N.A. Suslov, N.V. Frolova** Russian Federal Nuclear Centre – All-Russian Research Institute of Experimental Physics, prosp. Mira 37, 607190 Sarov, Nizhnii Novgorod region, Russia; e-mail: suslov@otd13.vniief.ru

sional knowledge about the symmetry of target implosion may be gained by way of recording a 'voluminal' (tomographic) image of the object. The methods of obtaining such images have been well elaborated and are most extensively used in medicine [2]. To obtain a tomographic image of an object in transmitted or intrinsic radiation, a large number of its two-dimensional images are recorded along different directions. The three-dimensional distribution of object characteristics is reconstructed from the 2D images using mathematical techniques. The tomographic image of the object permits acquiring the distribution of its characteristics at an arbitrary section through the object or determining the shape of the surface inside the object which corresponds to any signal level.

Several examples of applying computer tomography to laser fusion research are known from the literature [3].

2. Experimental conditions and execution of measurements

The technique of recording the tomographic image of a microtarget directly irradiated by the second harmonic of iodine laser radiation ($\lambda \approx 0.66$ μm) was implemented in experiments on the Iskra-5 facility [4]. The microtarget was a glass spherical shell with a diameter of 513 μm and a wall thickness of 1.3 μm, which was filled with a DT mixture to a pressure $p_{DT} = 3$ atm. The laser radiation with a total energy of 2.7×10^3 J was focused to a spot of diameter ~ 160 μm on the target surface, which knowingly produced a relatively nonuniform shell irradiation. In this case, the average intensity of laser irradiation of the target surface was 4.6×10^{14} W cm^{-2} for a laser pulse duration of ~ 0.6 ns.

To obtain the tomographic image of the microtarget, we made use of a set of microtarget images in its intrinsic X-ray radiation. The images were produced by seven pinhole cameras arranged evenly enough around the microtarget on the flanges of the upper and lower hemispheres of the vacuum chamber of the Iskra-5 facility. Each pinhole camera had a set of openings with diameters of $9 - 30$ μm. By and large, these opening diameters afforded a wide dynamic range of recording ($\sim 10^3$). The images were recorded with a $4.3 - 4.6$ fold magnification on UF-4 photographic film.

For filters we employed 20-μm thick beryllium foils. These filters are 'grey' and have a cutoff energy of 1.5 keV, and the images are therefore formed by the radiation with a rather broad spectrum. To convert film blackening densities

to X-ray photon densities, we reconstructed the characteristic curve of the film by comparing two images recorded behind the openings of different diameter.

In the tomographic image reconstruction we processed all images recorded from different directions, and so their brightnesses were corrected to take into account the specific diameters of pinhole camera openings, the distances, and the magnification coefficients. According to our estimates, the resultant uncertainty of binding the images in brightness was within $\pm 20\%$.

An important point in the reconstruction of a tomographic image is correct mutual spatial referencing of the images recorded from different directions. The centre of a circle circumscribed about the apparent shell contour was adopted as the centre of the images. According to our estimates, the position of the centre in the microtarget plane was determined accurate to $\sim 5\ \mu m$. To obtain angular referencing of the images, we carried out an additional (calibration) experiment involving irradiation of a glass fibre by the radiation of four channels of the facility, so that the image of the fibre was seen from all seven directions of observation. The invariable angular orientation of aperture stops in the course of the principal and calibration experiments, the well-known geometry of the arrangement of the series of openings in the aperture stops of multichannel pinhole cameras, as well as using a fibre as the target in the calibration experiment to unambiguously define a certain spatial direction, allowed us to determine the angular orientation of the images relative to each other. An analysis showed that the uncertainty of angular image referencing with the use of the above method was within $1°$.

The images recorded experimentally are given in Table 1. One can see that the shell glow is nonuniform. Clearly seen in all images is the glow of the compressed domain at the shell centre, which is complex in shape. The

Table 1. Comparison of two-dimensional microtarget images upon reconstruction with experimental results.

s	θ/deg	φ/deg	Two-dimensional images	
			Experiment	Calculation
1	43	−10		
2	43	−80		
3	43	170		
4	43	100		
5	137	−135		
6	137	135		
7	137	45		

N o t e. Angles θ and φ define the direction of observation by pinhole cameras in the spherical coordinate system.

shadow of a shell suspension filament is seen in the images which were obtained with the pinhole cameras located in the upper hemisphere.

3. Three-dimensional tomographic image reconstruction

The problem of reconstructing the internal structure of an object from a small number of its projections (few-view tomography) belongs to the class of so-called ill-posed problems. This is due to the fact that the number of unknowns in such a problem is proportional to N^3, where N is the dimension (partition number) of a domain which encompasses the three-dimensional object under investigation, while the number of known quantities is proportional to kN^2, where k is the number of projections (perspective angles). As a consequence, for $k < N$ the system of equations turns out to be essentially underdetermined. Therein lies the difference between few-view tomography and conventional medical tomography, in which the number of projection angles may be sufficiently large.

In our experiments, the reconstruction was performed from the resultant two-dimensional images, each of which was the integral of the sought-for object luminosity taken along a specific observation direction. Every element of the image array was assumed to be the integral of the luminosity of the sought-for three-dimensional object taken along a narrow ray (Fig. 1). The reconstruction algorithm applied in our work was based on the method of successive approximations. By using this method, in the three-dimensional reconstruction domain it is possible to select the luminosity distribution in such a way as to minimise the quadratic residual (function) between the given and calculated two-dimensional images. On the strength of the underdeterminedness of the system of equations, such a luminosity distribution may not be unique.

The problem of reconstruction of three-dimensional objects from their projections reduces to the solution of the integral equation

$$m_s(\boldsymbol{r}_0) = \int_{V_{tg}} \mu(\boldsymbol{e}_s\tau + \boldsymbol{r}_0)\mathrm{d}\tau, \tag{1}$$

where $\mu(\boldsymbol{r})$ is the sought-for object luminosity at point $\boldsymbol{r}$; $m_s(\boldsymbol{r}_0)$ is the ray sum determined on the object image at point $\boldsymbol{r}_0$ for the sth projection direction; $\boldsymbol{e}_s$ is the unit vector in the direction of observation; and τ is the distance of the recording plane to the point $\boldsymbol{r}$; the integration is performed over the volume V_{tg} of the object under investigation.

In the execution of numerical calculations, the integral is replaced by the system of linear equations

$$m_{sgl} = \sum_i \sum_j \sum_k V_{ijksgl}\mu_{ijk},$$
$$i,j,k,g,l = 1,...,200, \quad s = 1,...,7, \tag{2}$$

where the indices g, l define the coordinates of an element of the object image in the recording plane for the sth projection, and the indices i, j, k define the coordinates of an element of the object; V_{ijksgl} is the 'weight' coefficient (see Fig. 1), which is the volume intercepted by the projection ray in the element of the spatial object mesh.

The three-dimensional object reconstruction was performed using a code which made use of additional
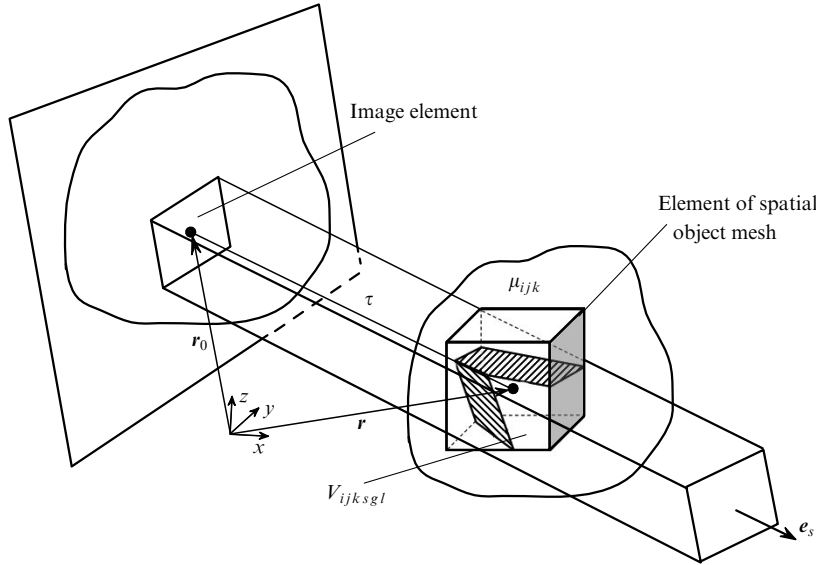
Figure 1. Illustration of the physical meaning of the weight coefficients in ray sums.

information contained in the first derivatives of the function $m_s(r_0)$ so as to reduce the underdeterminedness of the initial data and improve the reconstruction quality. In the reconstruction, the dimensionality of the matrix of the reconstruction domain was $200 \times 200 \times 200$ elements, while the dimensionality of the matrices of two-dimensional images was 200×200 elements. A circular mask of diameter 1.25 times the microtarget diameter was imposed on the given (experimentally obtained) two-dimensional images. Outside this circle the image intensity was assumed to be zero. This enabled us to accurately take into account the glow of the plasma that expanded beyond the confines of the microtarget. The reconstruction was executed neglecting the absorption of radiation in the target volume.

Table 1 gives the images recorded in experiment and those calculated upon image reconstruction. One can see that these images are hardly different when inspected visually.

The reconstructed projections of the compressed central domain in three orthogonally related directions are shown in Table 2 at a level of half the peak intensity of the glow. The compressed domain at the target centre is complex in shape. Structural elements measuring $20 - 30$ μm are easily discernible in the image of this domain, and its brightest part is displaced by ~ 30 μm from the target centre.

A neutron yield $Y_n = 2 \times 10^8$ was recorded in the experiment.

As noted above, tomographic imaging permits gaining information about any fragment of a microtarget. Voluminal plasma luminosity may be integrated along the radius to some depth to obtain the function $\Phi(\theta, \varphi)$, which reflects the spatial distribution of surface irradiance. In this case it is assumed that the X-ray radiation intensity is directly proportional to the laser irradiation intensity. The distribution $\Phi(\theta, \varphi)$ obtained by integrating the shell plasma luminosity over depth up to $R = 0.5R_{tg}$, where $0.5R_{tg}$ is the approximate radius to which the shell compressed during the course of a laser pulse, is depicted in Fig. 2. One can see that four–five brightest-radiating domains stand out on the shell surface instead of the twelve expected ones, and some domains are hardly irradiated at all.
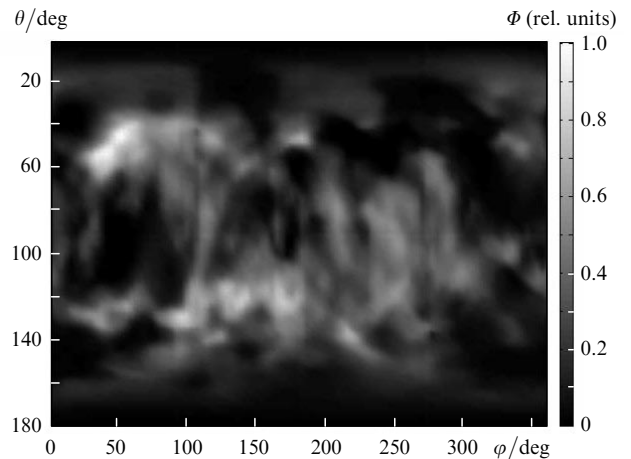

Figure 2. Reconstructed angular distribution $\Phi(\theta, \varphi)$ of shell irradiance.

The characteristic spatial nonuniformity scale lengths in the distribution $\Phi(\theta, \varphi)$ may be analysed by application of harmonic analysis. The parameter

$$\varepsilon_n = \left[\alpha_{n0}^2 + \sum_{m=1}^{n} \left(\alpha_{nm}^2 + \beta_{nm}^2 \right) \right]^{1/2}, \qquad (3)$$

being proportional to the coefficients α_{n0}, α_{nm} and β_{nm} of expansion of the normalised distribution $\tilde{\Phi}(\theta, \varphi)$ in terms of the complete system of normalised spherical harmonics of
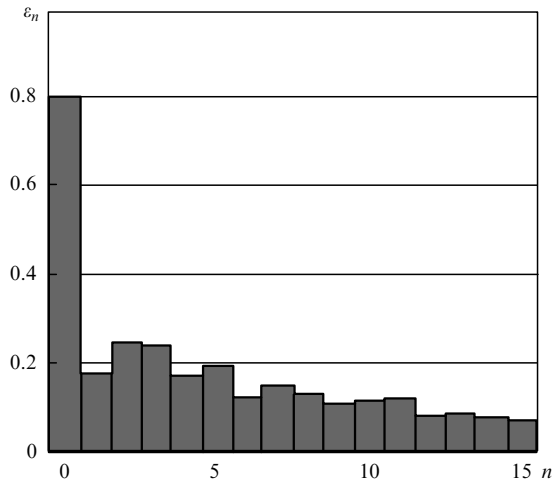
Table 2. Principal projections of the reconstructed compressed domain.

Reconstruction scheme	Top view	Front view	Right-side view
	250 μm	250 μm	250 μm

Figure 3. Values of parameter ε_n calculated from the $\Phi(\theta, \varphi)$ distribution for spherical harmonics of order n.

References

1. Lind J. *Phys. Plasmas*, **2**, 3933 (1995).
2. Herman G.T. *Image Reconstruction from Projections. The Fundamentals of Computerized Tomography* (New York: Academic Press, 1980).
3. Nishimura H., Niki H., Miyanaga N., et al. *Rev. Sci. Instr.*, **56**, 1128 (1985).
4. Annenkov V.I., Bessarab A.V., Vatulin V.V., Zhidkov N.V., et al. *Proc. XXIX ECLIM* (Madrid, Spain, 2006) pp 62–67.

order n, characterises the contribution of these harmonics to the $\Phi(\theta, \varphi)$ distribution. It is a rotational invariant and may be considered as a characteristic of the nonuniformity in the irradiance distribution. Figure 3 depicts the values of ε_n for the distribution $\Phi(\theta, \varphi)$.

It is evident that by and large the contribution of harmonics to the irradiance distribution becomes smaller with increasing the harmonic order. The zero harmonic is most intense, most intense among the remaining harmonics are the second and third ones. The rms nonuniformity of shell irradiance is equal to $\sim 60\,\%$.

4. Conclusions

In an experiment carried out on the twelve-channel Iskra-5 laser facility which involved direct irradiation of a spherical microtarget by the second harmonic of iodine laser radiation, we have implemented a method for recording its X-ray tomographic image. The tomographic image was reconstructed from seven two-dimensional microtarget images recorded in the X-ray radiation with photon energies above 1.5 keV from different directions, with the use of pinhole cameras. The projections of the reconstructed tomographic image are hardly different from the initial images recorded in the experiment.

From the reconstructed tomographic image it is evident that the shell surface was nonuniformly irradiated by laser radiation in the experiment conducted. In the expansion of target irradiance in terms of spherical harmonics, the zero harmonic is most intense, the second and third harmonics are the most intense among the remaining ones. The rms nonuniformity of target irradiance is estimated at $\sim 60\,\%$. The reconstructed compressed domain is complex in shape. Structural elements measuring $20-30\ \mu m$ are clearly seen in it.